The Distinct Effects of Homogeneous Weak Disorder and Dilute Strong Scatterers on Phase Competetion in the Manganites

Kalpataru Pradhan, Anamitra Mukherjee and Pinaki Majumdar

Harish-Chandra Research Institute, Chhatnag Road, Jhusi, Allahabad 211 019, India

(Dated: 11 Aug, 2007)

We study the two orbital double-exchange model in two dimensions in the presence of antiferromagnetic (AF) superexchange, strong Jahn-Teller coupling, and substitutional disorder. At hole doping $x = 0.5$ we explore the 'bicritical' regime where the energy of a ferromagnetic metal and a charge and orbital ordered (CO-OO) CE state are closely balanced, and compare the impact of weak homogeneous disorder to that of a low density of strong scatterers. Even moderate homogeneous disorder suppresses the CE-CO-OO phase and leads to a glass with nanoscale correlations. Dilute strong scatterers of comparable strength, however, convert the CE-CO-OO phase to a *phase separated* state with ferromagnetic and AF-CO-OO clusters. We provide the first spatial description of these phenomena and compare our results in detail to experiments on the half-doped manganites.

The manganese oxides of the form $A_{1-x}A'_x MnO_3$ involve a remarkable interplay of charge, spin, lattice, and orbital degrees of freedom [1]. This cross coupling is most striking in the half doped ($x = 0.5$) manganites many of which have a charge and orbital ordered insulating (CO-OO-I) ground state with 'CE' magnetic order - a zigzag pattern of ferromagnetic chains with antiferromagnetic (AF) coupling between them. The CE-CO-OO-I phase shows up in manganites with low mean cation radius (r_A) while systems with large r_A are ferromagnetic metals (FM-M). The variation of r_A leads to a 'bicritical' phase diagram [2] with a first order boundary between the FM-M and the CE-CO-OO-I phases.

Disorder has a remarkable effect on the bicriticality. Even moderate 'alloy' disorder, due to random location of A and A' ions at the rare earth site, converts the CO-OO-CE phase to a short range correlated glass, but has only limited impact on the ferromagnet [2, 3, 4]. The asymmetric suppression of spatial order by cation disorder and the emergence of a charge-orbital-spin glass at low r_A are one set of intriguing issues in these materials. Unusually, while alloy type randomness on the A site leads to a *homogeneous glassy phase*, the substitution of a few percent of Mn (the 'B site') by Cr [5, 6] leads to *phase separation* of the system [7, 8, 9, 10] into FM-M and AF-CO-OO-I domains. The difference between A and B site disorder holds the key to the much discussed phase coexistence and spatial inhomogeneity in the manganites.

In this paper we provide the first results on the relative effects of A and B type substitutional disorder on phase competetion in a manganite model. We study weak 'alloy' disorder and dilute strongly repulsive scatterers. Our main results are: (i) Alloy disorder indeed leads to asymmetric suppression of long range order; moderate disorder converts long range CE-CO-OO to an *insulating glass* with nanoscale inhomogeneities, while FM order is only weakened. (ii) A low density, $\gtrsim 4\%$, of strong scatterers in the CE phase leads to cluster coexistence of AF-CO-OO and FM regions and the ground state is a *poor metal*.

(iii) The impact of strong scatterers depends crucially on whether they are attractive or repulsive, it correlates with the asymmetry of the 'clean' system about $x = 0.5$, and uncovers a new route for phase control.

We consider a two band model for e_g electrons, Hunds coupled to t_{2g} derived core spins, in a two dimensional square lattice. The electrons are also coupled to Jahn-Teller phonons, while the core spins have an AF superexchange coupling between them. These ingredients are all necessary to obtain a CE-CO-OO phase. We include the effect of disorder through an on site potential.

$$H = \sum_{\langle ij \rangle \sigma}^{\alpha\beta} t_{\alpha\beta}^{ij} c_{i\alpha\sigma}^\dagger c_{j\beta\sigma} + \sum_i (\epsilon_i - \mu) n_i - J_H \sum_i \mathbf{S}_i . \boldsymbol{\sigma}_i$$
$$+ J_{AF} \sum_{\langle ij \rangle} \mathbf{S}_i . \mathbf{S}_j - \lambda \sum_i \mathbf{Q}_i . \boldsymbol{\tau}_i + \frac{K}{2} \sum_i \mathbf{Q}_i^2. \quad (1)$$

Here, c and $c^\dagger$ are annihilation and creation operators for e_g electrons and α, β are the two Mn-e_g orbitals $d_{x^2-y^2}$ and $d_{3z^2-r^2}$, labelled (a) and (b) in what follows. $t_{\alpha\beta}^{ij}$ are hopping amplitudes between nearest-neighbor sites with the symmetry dictated form: $t_{aa}^x = t_{aa}^y \equiv t$, $t_{bb}^x = t_{bb}^y \equiv t/3$, $t_{ab}^x = t_{ba}^x \equiv -t/\sqrt{3}$, $t_{ab}^y = t_{ba}^y \equiv t/\sqrt{3}$, where x and y are spatial directions We consider effectively a lattice of Mn ions and treat the alloy disorder due to cationic substitution as a random potential ϵ_i at the Mn site picked from the distribution $P_A(\epsilon_i) = \frac{1}{2}(\delta(\epsilon_i - \Delta) + \delta(\epsilon_i + \Delta))$. The Cr doping case is modelled via $P_B(\epsilon_i) = \eta\delta(\epsilon_i - V) + (1 - \eta)\delta(\epsilon_i)$, where η is the percent substitution and V the effective potential at the impurity site. The e_g electron spin is $\sigma_i^\mu = \sum_{\sigma\sigma'}^\alpha c_{i\alpha\sigma}^\dagger \Gamma_{\sigma\sigma'}^\mu c_{i\alpha\sigma'}$, where the Γ's are Pauli matrices. It is coupled to the t_{2g} spin $\mathbf{S}_i$ via the Hund's coupling J_H, and we assume $J_H/t \gg 1$. λ is the coupling between the JT distortion $\mathbf{Q}_i = (Q_{ix}, Q_{iz})$ and the orbital pseudospin $\tau_i^\mu = \sum_\sigma^{\alpha\beta} c_{i\alpha\sigma}^\dagger \Gamma_{\alpha\beta}^\mu c_{i\beta\sigma}$, and K is the lattice stiffness. We set $t = 1$, $K = 1$, and treat the $\mathbf{Q}_i$ and $\mathbf{S}_i$ as classical variables [11]. The chemical potential μ is adjusted so that the electron density remains $n = 1/2$ which is also $x = 1 - n = 1/2$. For A
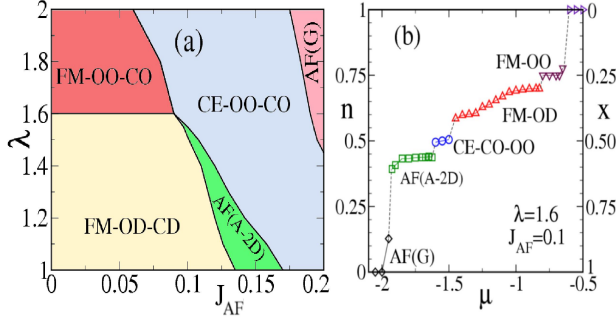
FIG. 1: Colour online: (a) The ground state at $x = 0.5$ for varying J_{AF} and λ, in the absence of disorder. (b) The doping ($n = 1 - x$) dependence of the ground state for varying chemical potential μ and typical electronic couplings, $\lambda = 1.6$ and $J_{AF} = 0.1$, near the FM-OD-CD & CE-CO-OO phase boundary. The phases in the vicinity of $x = 0.5$ are expected to show up in a cluster pattern on introducing disorder at $x = 0.5$.
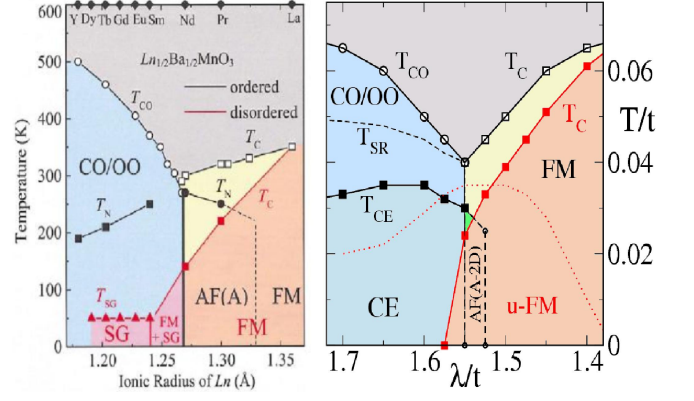

FIG. 2: Colour online: (a) Experimental 'bicritical' phase diagram in the $x = 0.5$ manganites obtained for ordered and disordered (alloy) structures. (b) Our results: superposed phase diagrams at $x = 0.5$ for $\Delta = 0$ and $\Delta = 0.3$. The long range CE-CO-OO for $\lambda > 1.55$ at $\Delta = 0$ is completely wiped out at $\Delta = 0.3$ while the FM-M phase at low λ becomes an unsaturated FM with short range A-2D type correlations.

type disorder the mean value is $\bar{\epsilon}_i = 0$ and the variance is $\Delta_A^2 = \langle (\epsilon_i - \bar{\epsilon}_i)^2 \rangle = \Delta^2$, while for B type disorder $\bar{\epsilon}_i = \eta V$ and $\Delta_B^2 = \langle (\epsilon_i - \bar{\epsilon}_i)^2 \rangle = V^2 \eta (1 - \eta)$.

The clean CE ground state at $x = 0.5$ has been studied earlier [12, 13, 14, 15, 16] using mean field and Monte Carlo (MC) techniques and is well understood. The impact of disorder on the phase competetion appropriate to $x = 0.5$ has been studied on small clusters [17, 18, 19] usually using simplified models either without orbital variables [18] or ignoring the electron-phonon coupling [19]. The difficulty of simulating the full model, eqn[1], on a large system has prevented any conclusive study. We use our recently developed travelling cluster approximation (TCA) based MC [20] to solve the problem. Compared to exact diagonalisation (ED) based MC which can handle typical sizes $\sim 8 \times 8$ we study the full model on lattices upto 40×40. In all our studies we use a moving cluster of size $\sim 8 \times 8$ [20] to anneal the spin and phonon variables.

Before discussing the effect of disorder we determine the clean ground state at $x = 0.5$ for varying J_{AF} and λ, Fig.1.(a).

At low λ and low J_{AF} double exchange is the dominant interaction and kinetic energy optimisation leads to a homogeneous ferromagnetic state without any orbital or charge order (FM-OD-CD). This phase has a finite density of states at the Fermi level ϵ_F and is metallic. As J_{AF} is increased, keeping the JT coupling small, a magnetic state emerges with peaks in the structure factor $S_{mag}(\mathbf{q})$ at $\mathbf{q} = \{0, \pi\}$ or $\{\pi, 0\}$ (we call this the A-2D phase), then an orbital ordered but uniform density CE phase, with simultaneous peaks at $\mathbf{q} = \{0, \pi\}, \{\pi, 0\}$, and $\{\pi/2, \pi/2\}$. At even larger J_{AF} the dominant correlations are 'G type' with a peak at $\mathbf{q} = \{\pi, \pi\}$. By contrast, increasing λ at weak J_{AF} keeps the system fer-

romagnetic but leads to charge and orbital order (FM-CO-OO) for $\lambda \gtrsim 1.6$. Our interest is in a *charge ordered* CE phase. Such a state shows up when both λ and J_{AF} are moderately large. The TCA based phase diagram is broadly consistent with previous variational results [12, 14, 15, 16] and with ED-MC on small systems [13].

Since the effect of disorder might be to create cluster coexistence [21, 22] of phases *of different densities* that arise in the clean limit, Fig.1.(b) shows the phases and phase separation windows that occur at a typical coupling, $J_{AF} = 0.1$ and $\lambda = 1.6$. For these couplings the clean system is a CE-CO-OO phase at $x = 0.5$, a FM-M for $x \lesssim 0.4$, and an A-2D type AF for $x \gtrsim 0.55$.

To minimise the number of parameters, in what follows we set $J_{AF} = 0.1$. This is in the right ballpark considering the AF transition temperature at $x = 1$, and allows close proximity of the CE and FM-M phases. We mimic the bandwidth variation arising from changing r_A by varying λ/t across the boundary between CE-CO-OO and FM-OD-CD, and now explore the effects of thermal fluctuation and disorder.

The key experiment [2] on the effect of A site disorder on bicriticality compared an 'ordered' structure, where the rare earth and alkaline earth ions *sit on alternate layers*, with the 'disordered' case where they are randomly distributed. The result is reproduced in the left panel in Fig.2. While the ordered case has large transition temperatures for the CO-OO, CE, FM phases, *etc*, a random distribution of A and A' ions destroy the CO-OO-CE phase and partially suppresses the ferromagnetic T_c.

The right panel in Fig.2 shows our result, where we superpose the clean phase diagram and the case with A
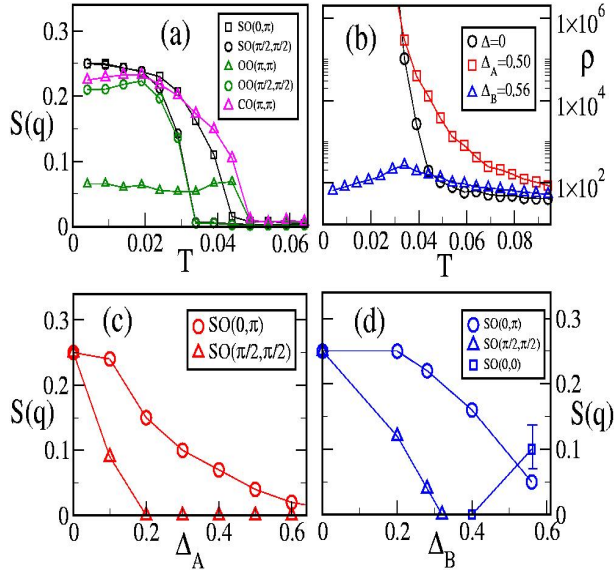
FIG. 3: Colour online: Structure factors and resistivity at $J_{AF} = 0.1$ and $\lambda/t = 1.6$. (a) The T dependence of the major peaks in the structure factor for spin order (SO), orbital order (OO) and charge order (CO) in the clean limit. Note the clear separation of scales between T_{CO}, T_{SR} and T_{CE}. (b) The resistivity $\rho(T)$ in the clean CE-CO-OO case and in the presence of A type and B type disorder, with $\Delta_A \approx \Delta_B \sim 0.5$. The Δ_B corresponds to $V = 2$ and dilution $\eta = 0.08$. (c) Variation of the major peaks in the magnetic structure factor with Δ_A at low temperature ($T = 0.005$). (d) Same as (c), now with B type disorder, $V = 2$ and varying η. Note the emergence of the FM $\mathbf{q} = \{0, 0\}$ peak around $\Delta_B = 0.4$ ($\eta = 0.04$).

FIG. 4: Colour online: MC snapshots and magnetic structure factor at low temperature, $T = 0.01$, size 40×40. Left row: $\lambda = 1.6$, non disordered, middle row, $\lambda = 1.6$, A type disorder with $\Delta_{eff} = 0.5$, right row, $\lambda = 1.6$, B type disorder with $V = 2$, $\eta = 8\%$, $\Delta_{eff} = 0.56$. Top panel shows the nearest neighbour magnetic correlation $\mathbf{S}_i.\mathbf{S}_{i+\delta}$, where $\delta = x$ or y. Middle panel shows the charge density $\langle n_i \rangle$ for the configuration above. Bottom panels shows the MC averaged $S_{mag}(\mathbf{q})$. In each panel $\mathbf{q} = \{0, 0\}$ at the bottom left corner, $\mathbf{q} = \{\pi, 0\}$ at the bottom right corner, *etc.*

type disorder $\Delta_A = 0.3$. In the clean limit at $T = 0$ as λ/t is increased there is a transition from a FM-M to the A-2D phase at $\lambda/t \sim 1.52$, and then a transition to a CE-CO-OO phase at $\lambda/t \gtrsim 1.55$. On the FM-M side, $\lambda/t \leq 1.52$, there is only a single thermal transition [23] at T_C as one cools the system. At large λ/t, however, cooling first leads to a CO-OO phase, at T_{CO}, without magnetic order, followed by strong features in S_{mag} at $\mathbf{q} = \{0, \pi\}$ and $\{0, \pi\}$, showing up at T_{SR}, indicative of stripelike correlations. Finally, at a lower T the system makes a transition to CE order. If we set $t = 0.3$eV, and use a factor of $3/2$ to convert transition scales between 2D and 3D, our T_C at bicriticality would be ~ 200K.

In the presence of A type disorder with $\Delta_A = 0.3$ we do not find any spatial order on the CE side in either the charge, or orbital, or magnetic sector, down to $T \sim 0.005$. The absence of order in the CE-CO-OO side can be traced back to the 'random field' ϵ_i coupling directly to the charge order parameter n_i. This breaks down charge correlations to the atomic scale. The ferromagnet being a $\mathbf{q} = 0$ state is more robust to A type disorder [18].

There are short range stripelike magnetic correlations that persist as peaks at $\mathbf{q} = \{0, \pi\}$ and $\{\pi, 0\}$ in $S_{mag}(\mathbf{q})$.
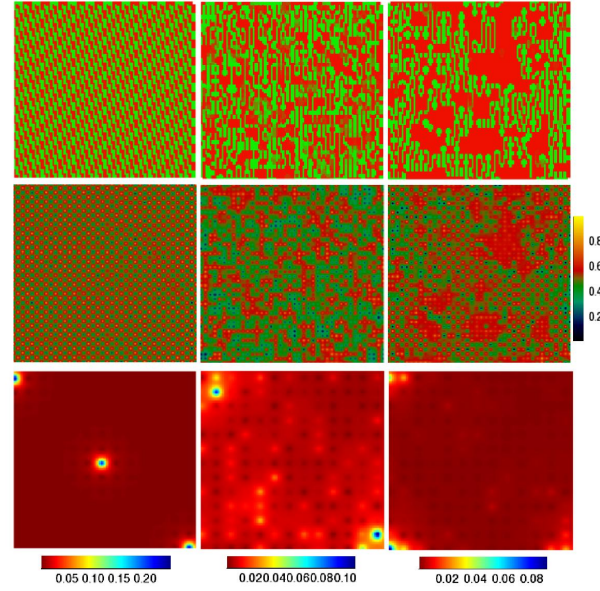
The onset of this feature is shown by the (red) dotted line in Fig.2.(b). This appears even on the ferromagnetic side below T_C. The T_C itself is somewhat suppressed by disorder and the ground state is an *unsaturated* ferromagnet (u-FM). Our analysis of the structure factor in the disordered system, however, does not suggest any coexistence of two distinct locally ordered phases at any λ. *A type disorder in the bicritical regime does not induce phase coexistence.* We have confirmed this directly from the spatial snapshots as well, as we discuss later.

We have explored A type disorder with strength $\Delta_A = 0.1$, 0.2, 0.3 and 0.4, over the range of λ/t shown in Fig.2.(b). We now specialise to $\lambda/t = 1.6$, which is a CE-CO-OO phase near the clean phase boundary in Fig.2.(b) and explore the impact of A type and B type disorder in detail. Fig.3.(a) shows the T dependence of the major peaks in the spin, charge and orbital structure factor in the clean limit at $\lambda/t = 1.6$, for reference, illustrating the distinct T_{CO}, T_{SR} and T_{CE} scales.

The naive expectation is that disorder would lead to cluster coexistence [21, 22] of AF-CO phases, that arise for $x \geq 0.5$, with the FM-M phase at $x \lesssim 0.4$, Fig.1.(b). Fig.3.(c) shows how the peaks in $S_{mag}(\mathbf{q})$ evolve with Δ_A at low temperature ($T = 0.01$). The peak at $\mathbf{q} = \{\pi/2, \pi/2\}$ vanishes quickly, leading to a phase with

stripelike correlations, and the $\mathbf{q} = \{0, \pi\}$, $\{\pi, 0\}$ peaks also vanish for $\Delta_A > 0.6$ leaving a glass. The response to B type disorder is more interesting. We have explored $V = 1$, 2 and 4 and $\eta = 2$, 4 and 8%. Since Cr is believed to be in a $t_{2g}^3 e_g^0$ state we focus here on $V = 2$ which is sufficiently repulsive to force $\langle n_i \rangle = 0$ (e_g^0 state) at the impurity sites. The response, as we vary the fraction of scatterers (η), is similar to A type at weak Δ_B. However, before the peak at $\mathbf{q} = \{0, \pi\}$, $\{\pi, 0\}$ vanishes we see the emergence of a peak at the ferromagnetic wavevector, $\mathbf{q} = \{0, 0\}$. There is a window at intermediate η where *B type disorder leads to coexistence of FM and CO-OO-AF regions*. In terms of transport, Fig.3.(b), intermediate A type disorder strengthens the insulating character in $\rho(T)$, while B type disorder of comparable variance leads to an insulator-metal transition on cooling, and a (poor) metallic state at low temperature.

The top row in Fig.4 compares low temperature MC snapshots of the magnetic correlations in the clean system at $\lambda = 1.6$ (left), to that with $\Delta_A = 0.5$ (center) and $\Delta_B = 0.56$ (right). The respective panels in the middle row show the electron density $\langle n_i \rangle$ corresponding to the panels above. The panels at the bottom are the thermally averaged $S_{mag}(\mathbf{q})$ in the three cases. In the clean limit the magnetic correlations are CE, with a checkerboard density distribution, and simultaneous magnetic peaks at $\mathbf{q} = \{0, \pi\}$, $\{\pi, 0\}$ and $\{\pi/2, \pi/2\}$. For A type disorder there are stripelike magnetic correlations with small (atomic scale) FM clusters but no signature of phase coexistence. The density field is also inhomogeneous in the nanoscale, with only short range charge correlations, and $S_{mag}(\mathbf{q})$ has weak peaks at $\mathbf{q} = \{0, \pi\}$ and $\{\pi, 0\}$ but no noticeable feature at $\mathbf{q} = \{0, 0\}$. B type disorder, however, leads to FM *regions* coexisting with stripelike AF correlations. The density field shows a corresponding variation, being roughly homogeneous within the FM droplets (with local density $n \sim 0.6$), and a CO pattern away from the FM regions. $S_{mag}(\mathbf{q})$ now has peaks at $\mathbf{q} = \{0, \pi\}$, $\{\pi, 0\}$ *and* $\{0, 0\}$, as seen earlier in Fig.3.(d).

We explain the difference between the impact of A type and B type disorder as follows. (1) The introduction of A type disorder does not lead to coexistence of large FM-M and AF-CO-OO clusters, despite the presence of a PS window in the clean problem, Fig.1.(b), because (a) atomic scale potential fluctuations disallow CO coherence beyond a few lattice spacings, while (b) homogeneous FM-M clusters are destabilised by the disorder and become charge modulated. The result is a nanoscale correlated insulating glassy phase. (2) Dilute strongly repulsive scatterers act very differently: (a) they force an e_g^0 state at the impurity sites and generate an 'excess density' $0.5 \times \eta$ which has to be distributed among the remaining Mn sites, (b) the parent $x = 0.5$ CO phase cannot accommodate this excess charge homogeneously and the system prefers to phase separate into $x \sim 0.5$ AF-CO and $x \sim 0.4$ FM clusters, (c) unlike the A type case, the

FM clusters can survive and percolate since at low η there can be *large connected patches* without a B type site. We have verified this explicitly for several impurity configurations. Making the B site potential *strongly attractive* leads to a glassy AF-CO state since carrier trapping reduces the effective electron count and forces the system towards a combination of $x \geq 0.5$ phases in Fig1.(b).

In conclusion, we have reproduced all the key effects of A and B type disorder on phase competetion in the half doped manganites. Our results suggest that B site impurities can be chosen to engineer phase control and the percolative conduction paths can be controlled through choice of dopant locations.

[1] See, *e.g*, *Colossal Magnetoresistive Oxides*, edited by Y. Tokura, Gordon and Breach, Amsterdam (2000).
[2] D. Akahoshi, *et al.*, Phys. Rev. Lett. **90**, 177203 (2003).
[3] R. Mathieu, *et al.*, Phys. Rev. Lett. **93**, 227202 (2004).
[4] Y. Tokura, Rep. Prog. Phys. **69**, 797 (2006).
[5] A. Barnabe, *et al.*, Appl. Phys. Lett. **71**, 3907 (1997).
[6] B. Raveau, *et al.*, J. Solid State Chem. **130**, 162 (1997).
[7] T. Kimura, *et al.*, Phys. Rev. Lett. **83**, 3940 (1999).
[8] T. Kimura, *et al.*, Phys. Rev. **B62**, 15021 (2000).
[9] H. Oshima, *et al.*, Phys. Rev. **B63**, 094420 (2001).
[10] S. Mori, *et al.*, Phys. Rev. **B67**, 012403 (2003).
[11] The validity of the classical approximations is studied in, *e.g*, E. Dagotto, *et al.*, Phys. Rev. **B 58**, 6414 (1998) and A. C. Green, Phys. Rev. **B 63**, 205110 (2001).
[12] J. van den Brink *et al.*, Phys. Rev. Lett. **83**, 5118 (1999).
[13] S. Yunoki, *et al.*, Phys. Rev. Lett. **84**, 3714-3717 (2000).
[14] L. Brey, Phys. Rev. **B 71**, 174426 (2005).
[15] O. Cepas *et al.*, Phys. Rev. Lett. **94**, 247207 (2005).
[16] S. Dong, *et al.*, Phys. Rev. **B 73**, 104404 (2006).
[17] H. Aliaga, *et al.*, Phys. Rev. **B 68**, 104405 (2003).
[18] Y. Motome, *et al.*, Phys. Rev. Lett. 91, 167204 (2003)
[19] G. Alvarez, *et al.*, Phys. Rev. **B 73**, 224426 (2006).
[20] S. Kumar and P. Majumdar, Eur. Phys. J. **B 50**, 571 (2006).
[21] Adriana Moreo, *et al.*, Phys. Rev. Lett. **84**, 5568 (2000).
[22] S. Kumar and P. Majumdar, Phys. Rev. Lett. **92**, 126602 (2004).
[23] Our 2D magnetic "T_C" correspond to correlation length $\xi(T_C) \approx L$. There is no genuine T_C for $L \to \infty$ in 2D. The real 3D T_C will be $\approx 3/2$ times the 2D scale here.